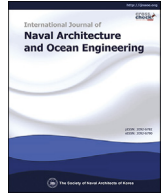




Contents lists available at ScienceDirect

International Journal of Naval Architecture and Ocean Engineering

journal homepage: <http://www.journals.elsevier.com/international-journal-of-naval-architecture-and-ocean-engineering/>

Marine gas turbine monitoring and diagnostics by simulation and pattern recognition

Ugo Campora^a, Carlo Cravero^a, Raphael Zaccone^{b,*}^a Dipartimento di Ingegneria Meccanica, Energetica, Gestionale, Trasporti (DIME), University of Genoa, Polytechnic School, Italy^b Dipartimento di Ingegneria Navale, Elettrica, Elettronica e delle Telecomunicazioni (DITEN), University of Genoa, Polytechnic School, Italy

ARTICLE INFO

Article history:

Received 2 September 2016

Received in revised form

10 August 2017

Accepted 13 September 2017

Available online 30 December 2017

Keywords:

Monitoring and diagnostics

Artificial neural networks

Ship simulation

Ship propulsion

Gas turbines

ABSTRACT

Several techniques have been developed in the last years for energy conversion and aeronautic propulsion plants monitoring and diagnostics, to ensure non-stop availability and safety, mainly based on machine learning and pattern recognition methods, which need large databases of measures. This paper aims to describe a simulation based monitoring and diagnostic method to overcome the lack of data. An application on a gas turbine powered frigate is shown. A MATLAB-SIMULINK® model of the frigate propulsion system has been used to generate a database of different faulty conditions of the plant. A monitoring and diagnostic system, based on Mahalanobis distance and artificial neural networks have been developed. Experimental data measured during the sea trials have been used for model calibration and validation. Test runs of the procedure have been carried out in a number of simulated degradation cases: in all the considered cases, malfunctions have been successfully detected by the developed model.

© 2017 Society of Naval Architects of Korea. Production and hosting by Elsevier B.V. This is an open access article under the CC BY-NC-ND license (<http://creativecommons.org/licenses/by-nc-nd/4.0/>).

1. Introduction

Real time operation monitoring and effective fault diagnosis are crucial issues in plant management, in order to increase safety and reliability. High availability, even if a fault occurs, is a desirable feature in almost any engineering application field. Several monitoring and diagnostic techniques have been developed, especially for industrial power plants and aeronautic propulsion systems. The general intent of these techniques is to monitor the plant's operation through a number of measures of an appropriate set of physical and thermodynamic parameters, then to identify one or more diagnostic variables through a model, which can be based on various computing techniques such as simulation, optimization algorithms, expert systems, response surfaces. The presented approach features a large use of simulation techniques, combined with Artificial Neural Networks (ANN) and Mahalanobis distance calculation (Taguchi and Jugulum, 2002), to obtain a fast and effective diagnosis for real-time applications. In the past years the authors gained significant experience in marine propulsion plants simulation (Benvenuto et al., 2000; Benvenuto and Campora, 2005;

Campora et al., 2013; Altosole et al., 2014), as well as in the application of ANN based metamodels for ship machinery diagnostics (Campora et al., 2015; Zaccone, 2013; Zaccone et al., 2015).

In these last studies, simulations were performed to generate a large amount of operational data, in order to overcome the lack of experimental measures. In addition, simulation helped to investigate the effects of component degradation, and ANN based metamodels were used in place of simulation to reduce computation time and allow problem inversion. The presented application is focused on the gas turbine-controllable pitch propellers propulsion plant of a frigate: a set of simulations in different working conditions has been carried out in order to obtain an exhaustive description of the plant behavior in all the operating and degradation states. Simulation results have been used to define a reference state of the plant, and Mahalanobis distance has been adopted in order to easily detect abnormal working conditions during plant's operation. In addition, the obtained database has been used to train a diagnostic artificial neural network, which provides the fault coefficients of the different plant components. In order to match the simulation database with the real plant's operation data, a calibration method has been applied.

2. Gas turbines diagnostics: an overview

Several approaches to fault diagnosis have been developed in

* Corresponding author.

E-mail address: raphael.zaccone@edu.unige.it (R. Zaccone).

Peer review under responsibility of Society of Naval Architects of Korea.

the last 50 years. Gas turbine powered systems diagnostic literature is wide and rich, especially in the aeronautic field. Li (2002) offers a review of the principal state-of-the-art techniques, analyzing a large number of papers by different authors, presenting a classification of the most used diagnostics and monitoring methods. According to Li, the approaches to the diagnostics problem can be divided into the following categories: linear model based methods, nonlinear model based methods, artificial intelligence based methods, fuzzy logic based methods.

Linear methods have been introduced by Urban (1969), using Gas Path Analysis (GPA): the purpose of the GPA is to extract information associated with the gas turbine engines via the analysis of the principal physical parameters of the plant, for example, pressures, temperatures, rotation speeds, flow rates, measuring them in different locations on the machinery. The GPA has been the most used approach to gas turbines monitoring and diagnostics in the last decades (Stamatis, 2011; Fentaye et al., 2016). In its most simplified form, the linear GPA, the highly nonlinear relationship between gas turbine dependent and independent parameters is simplified through a linear approximation at a given operating point (such as maximum power, cruise power, etc.). The paper by Verbist et al. (2011) shows an example of the application of linear GPA to a gas turbine engine. In order to overcome the problems due to the non-linear behavior of the gas turbine, nonlinear model based methods have been introduced. These methods are based on an accurate modeling of nonlinear gas turbine performance, combined with optimization techniques: the difference between measured and model predicted engine performance is minimized with an optimization approach in order to find the best set of engine component parameters. The artificial intelligence field is best referred as machine learning, or computational intelligence, with some slight semantic differences, however aims to mathematically reproduce biological systems architectures or behaviors such as neural systems, reproduction, human thinking or learning, in order to solve simpler problems. Artificial intelligence based methods are widely used in diagnostics applications: they are mainly based on Genetic Algorithms (GA), Expert Systems (ES), artificial neural networks (ANN), fuzzy logic. GA-based methods are model-based methods, theoretically similar to nonlinear model based. GAs are applied in the optimization phase, in order to identify a set of engine component parameters which produces the set of performance parameters that best matches the measured values. Expert systems are computer programs based on mainly experience knowledge (Bidini et al., 1998): an ES is composed of a knowledge base and an inference engine. The user interacts with the inference engine, which uses the knowledge base in order to solve problems and give advice: the solution of the problem is obtained through a heuristic type analysis. ANNs are based on the mathematical modeling of biological neural systems behavior, in order to store experimental knowledge contained in a database and to make it available for use. A brief description of ANN behavior can be found in a dedicated paragraph. In Palmé et al. (2011a) an ANN based system is used for gas turbine diagnostics: the ANN is trained using the experimental records of the first three months of operation of the plant, in order to obtain a model that can be used as a reference to the correct working condition. Other applications of auto-associative ANN in combination with principal component analysis are shown in Palmé et al. (2011b) and Kramer (1991). In the marine field, the authors presented an application of ANN to simulation and diagnostics of gas turbine and diesel engine powered marine propulsion plants (Campora et al., 2015), while Coraddu et al. (2016) presented an approach to marine gas turbines diagnostics based on statistical learning algorithms.

ANN applications to marine diesel engine diagnostics extensively discussed by Li and Su (2008) and Pawletko (2005), and later

in Zaccone et al. (2015).

Fuzzy logic based methods are also popular: fuzzy logic is an extension of the boolean logic theory, based on a ‘truth value’ between 0 and 1, which must not be confused with probability. Ogaji et al. (2005) show an application to gas turbine diagnostics using a GPA approach. Fuzzy logic can be applied in combination with neural networks, expert systems, genetic algorithms. Neuro-fuzzy approaches to diagnosis are described in Izadi-Zamanabadi et al. (2001) and Li and Su (2008) referring to gas turbines and marine diesel engines respectively. Finally, an effective diagnostic method based on the Mahalanobis - Taguchi system, combined with Bayesian networks and orthogonal arrays is presented in Kumano et al. (2011). The present work is based on this approach as described in the following.

3. Power plant monitoring and diagnostics procedure

The purpose of this paper is to present a procedure suitable for monitoring and diagnostics of energy conversion and propulsion plants. The procedure is structured on two monitoring levels: at a basic level, Mahalanobis Distance (MD) is used as an index of abnormality of the system; such parameter is computed from a set of state variables in order to compactly express the state of the system. The advantage of using only one parameter for system monitoring is obvious in terms of ease of representation and threshold setting. The robustness of such parameter to some external influences is shown in the paper. On a deeper monitoring level, if a high MD value is detected, a multi-input multi-output ANN based model is used in order to extract information on the state of each system component from the state variables.

3.1. The Mahalanobis distance

Mahalanobis Distance (MD) is a multivariate squared distance that takes in to account the variance and the correlation between the variables. In the framework of the Mahalanobis – Taguchi (MT) method (Taguchi and Jugulum, 2002), MD is used to quantify the abnormality of a generic condition of a multivariate system with respect to the ‘normal’ or ‘healthy’ condition, which is represented by a reference set of observations, called Mahalanobis Space (MS). The abnormality is measured by calculating the MD value for the actual condition. The advantage of using the MD instead of a different distance (for example the Euclidean distance) is the possibility to take into account the correlation between the variables.

Suppose the MS composed by n observations of k variables named X_1, \dots, X_k , n sufficiently large; if m_i and s_i are the means and the standard deviations of the variables respectively, C the correlation matrix of the variables, the MD of the j^{th} observation is given by the following expression:

$$MD_j = \left(\frac{1}{k}\right) Z_{ij}^T C^{-1} Z_{ij} \tag{1}$$

Where Z_{ij} is the i^{th} standardized variable for the j^{th} observation:

$$Z_{ij} = \frac{X_{ij} - m_i}{s_i} \tag{2}$$

Note that MD is a dimensionless squared distance. An alternative definition is used in Kumano et al. (2011), where the square root is used in order to eliminate the quadratic dependence. This last definition is used in this work:

$$MD_j = \sqrt{\left(\frac{1}{k}\right) Z_{ij}^T C^{-1} Z_{ij}} \tag{3}$$

The observation j does not need to be included into MS: in other words, once MS is defined, it is possible to calculate the MD for any condition. The standardized values of the generic observation j can be obtained using the means m_i and the standard deviations s_i obtained from the MS population, while the correlation matrix is fixed once the MS is defined.

It is possible to demonstrate that the mean of the MD of the MS elements equals unity (Taguchi and Jugulum, 2002). For a generic observation, a diagnosis can be made through MD calculation. A low MD value (close to 1) suggests the condition is normal (not far from the conditions chosen as the MS), while a high MD value points out an abnormality. So, the definition of the MS is crucial to obtain a correctly and usefully scaled MD.

In case the correlation matrix C is close to singularity, errors may occur while calculating the inverse matrix. Mahalanobis Taguchi Gram Schmidt method (MTGS) (Taguchi and Jugulum, 2002; Kumano et al., 2011) is helpful to overcome problems due to matrix singularity.

The MT/MTGS method has the advantage to combine all the information brought by a number of variables into one index, taking also into account the correlation matrix. In addition, it is required only simple matrix calculation to obtain a diagnosis. However, MD does not give any information on the variables of the system: to overcome that limitation, an Orthogonal Arrays (OA) analysis is suggested in Taguchi and Jugulum (2002), Kumano et al. (2011), in order to find out which variables are mainly responsible for a high (abnormal) MD value.

3.2. Artificial neural networks

Artificial neural networks are mathematical models based on the human brain structure, which are useful to solve a large number of problems, for instance, function fitting, clustering, classification, pattern recognition. The human brain is composed of a large number of elementary units (cells), called neurons, interconnected one to another by synapses. A neuron is a sort of filter, which receives a number of signals and activates if the total signal is higher than a threshold, sending its own signal to the other neurons. The information speed is not very high, but the neurons are massively parallel-connected, so the result is a very fast processing unit. A neuron (Fig. 1) can be mathematically modeled as a weighted summation block and an activation block: the input signals are collected into the array $\mathbf{x} = (x_1, \dots, x_n)$, while the vector $\mathbf{w} = (w_1, \dots, w_n)$ contains the weights. The summation block simply computes the value of the scalar product $a = \mathbf{x} \cdot \mathbf{w}$, which is compared to the threshold value θ . The output value $y = f(a - \theta)$ is calculated through the activation function f . There are several types of activation functions, the most commonly used are hard limit, sign function, linear, sigmoid, hyperbolic tangent. The choice of the activation function depends on the structure of the problem.

In analogy to the human brain, an ANN is composed of a large number of interconnected neurons, organized into three or more layers. The number of input and output layer neurons corresponds to the number of input/output parameters of the problem, while

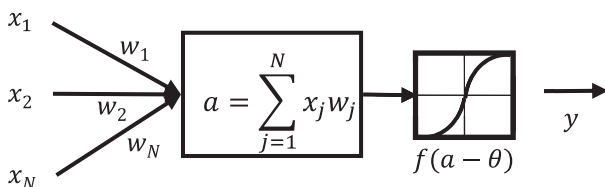


Fig. 1. Neuron model structure.

the number of neurons in the hidden layer(s) can be chosen on the basis of many different criteria (Campora et al., 2015; Zaccone et al., 2015; Rigoni and Lovision, 2007). An example of a three layers ANN with three inputs and two outputs is shown in Fig. 2. The advantage of using ANN is that there is no need to implement any description of the input/output relationship: the network ‘learns’ such a relationship from data. Once it is trained, an ANN is a black box that provides output values corresponding to any input pattern, so attention must be paid to ANN test and validation before trusting in network’s results. The learning process consists in the identification of the optimum weight values for each neuron. Learning is ‘supervised’ if input/output data is available, otherwise learning is said ‘unsupervised’ if only input data is available. Supervised learning for multilayer neural networks is based on the back-propagation algorithm: basically, for each element of the training set, the output of each neuron is computed (forward pass). An error signal is calculated subtracting the desired and predicted output values, and a weight correction is determined for each neuron back-propagating the error (backward pass). The learning is stopped when the error is found to be less than a threshold value. The performance of an ANN is usually evaluated through the Mean Square Error (MSE) which expresses the difference between the predicted output vector \mathbf{o} and target output vector \mathbf{t} . If the training set is made by N patterns, the MSE is given by:

$$MSE = \frac{1}{N} \sum_{i=1}^N (\mathbf{t}_i - \mathbf{o}_i)^2 \tag{4}$$

A detailed description of ANN and learning algorithms theory is brought by Haykin (1998).

4. Case study

The present application aims to predict the health state of a frigate propulsion plant and its components (mainly a gas turbine and two controllable pitch propellers driven by two shafts through a reduction gear). A brief description of the ship simulation model is presented hereinafter, however, further details can be found in Martelli et al. (2014a).

4.1. Ship propulsion plant scheme and physical principles-based simulation model

Fig. 3 shows the ship propulsion plant scheme with the fundamental components. The case study ship is 140 m long, displaces 5900 tons, and can achieve a maximum speed of 27 knots.

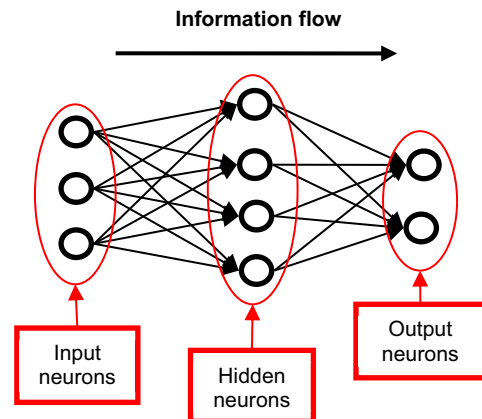


Fig. 2. An ANN composed by three layers.

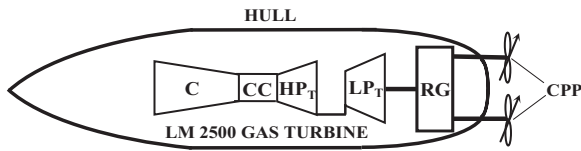


Fig. 3. Considered frigate propulsion plant scheme.

The main engine is the General Electric-AVIO LM 2500 Gas Turbine (GT), characterized by a two shafts arrangement. The gas generator is composed by the compressor (C in Fig. 3), the Combustion Chamber (CC) and the High-Pressure turbine (HP_T). The Maximum Continuous Rating (MCR) power, delivered by the power turbine (LP_T), is 32 MW at 3600 rpm. The power turbine drives two Controllable Pitch Propellers (CPP) via a cross-connecting Reduction Gearbox (RG), as discussed in Michetti et al. (2010).

The simulation model, fully described in Benvenuto and Campora (2005), is developed in a MATLAB-SIMULINK® environment and is organized in blocks, modeling the propulsion plant components (i.e. GT compressor and turbines, mechanical transmission, propeller and hull). Each component is modeled, on the basis of geometrical data, performance characteristics maps, physic and thermodynamic equations. The model allows simulating the performance of the propulsion plant in different load conditions and components health, in steady state and transient behavior.

A short description of the GT simulator is reported, while a more detailed explanation is presented in Benvenuto and Campora (2005).

For the compressor simulation (see MATLAB scheme of Fig. 4), typical steady state performance maps (Cohen et al., 1987) are used (Eff_table and Mair_table lookup tables in Fig. 4). The compressor efficiency (Eff_c) and the outlet air mass flow (Mair_c) are determined by the steady state performance maps, expressed as functions of the compressor pressure ratio ($\beta_{comp} = p_o/p_i$, Beta_Cmpr in Fig. 4) and shaft speed (N). The compressor behavior and functional data (i.e.: air mass flow and outlet temperature, shaft torque) are then easily computed by physics and thermodynamic dynamic equations. The gas generator shaft bearings losses are evaluated as a quadratic function of the compressor shaft speed. Compressor performance maps variation due to fouling, damage or fault are represented by means of the faults coefficients (K_{Ceff} and K_{CM} in Fig. 4). Finally, real compressor outlet temperature (T_{ro}) is determined from the outlet temperature in the case of isentropic compression (T_{iso}), by taking into account compressor efficiency, the required torque (Q_o) is calculated by considering the required

compression power (Power_Cmpr) and the shaft speed (N).

GT turbines performances (HP_T and LP_T in Fig. 3) are determined in a similar way. Degradation or fault of one or both the turbines is as well expressed through proper fault coefficients, which act on the performance maps.

The reduction gear (RG in Fig. 3) is simulated by a simple ratio between input and output rotating shafts speeds. The mechanical friction losses of the rotating shaft and the reduction gear are determined as in the gas generator shaft bearing loss case. The degradation of shaft bearings is taken into account by increasing the shaft mechanical friction torque via a proper coefficient.

The propeller model has been generated following the classical approach for the propeller performance prediction described in Altosole et al. (2012b), i.e. by using the propeller open water diagrams, in this application referred to a CPP.

The propellers thrust (K_T) and torque (K_Q) coefficients are determined from the open water diagrams, given the advance coefficient (J) and the propeller pitch diameter ratio (P/D) value. The dynamics of the pitch change mechanism is considered according to Altosole et al. (2012a) and Martelli et al. (2014b).

In the case of propeller fouling, damage or erosion, propellers coefficients are corrected through proper fault constants (Altosole et al., 2014), less than unity for K_T variation, and greater than unity for K_Q variation. In addition, an incorrect propeller blade angle, due to pitch actuator improper operation can be considered by the simulator code.

The frigate hull resistance is determined as a function of the ship speed, by a series of curves provided by the shipyard (Altosole et al., 2014). In particular, three resistance curves are provided, one referred the clean hull and two referred to increased surface roughness by fouling and corrosion, respectively after one and two years of in-water operation. The ship speed is determined by the dynamic balance equation between the hull resistance and propellers thrust forces (Benvenuto et al., 2000).

The overall propulsion plant governor is simulated in a proper module, whose functional scheme is reported in Fig. 5. A brief description of governor logic is reported, while a more detailed explanation is shown in Altosole and Martelli (2017).

As shown in Fig. 5, a demand lever (“telegraph”) placed on the command bridge on board, selects the propeller pitch value (P/D_{req} in the figure) and the rotational speed required to the engine (N_{ipT}). The ‘ship prop. system main governor’ module of Fig. 5 manages the P/D actuator and, by a PID governor system, the GT delivered power, through the required GT gas generator speed (N_{gg} in Fig. 5). This last signal is the input of the effective GT governor, named TCS (turbine control system) in Fig. 5. TCS manages the fuel valve position (FV_{pos}), in order to obtain the GT power to ensure the required GT

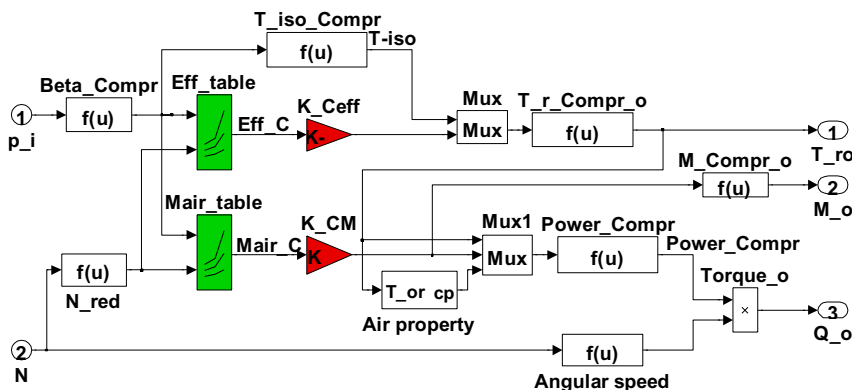


Fig. 4. Gas turbine compressor SIMULINK module.

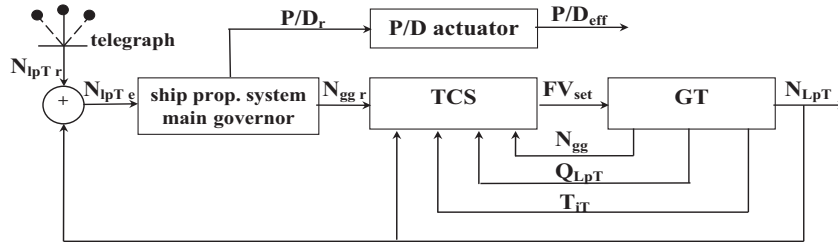


Fig. 5. Overall frigate propulsion control scheme.

power turbine speed. A complete propulsion plant scheme modelling is essential for a correct plant simulation performance under fault of one or more of its components. In fact, the TCS governor monitors a series of GT parameters [Altosole et al. \(2010\)](#). If, because of GT or propulsion plant components failure, one of the TCS monitored variables reaches the maximum allowable value, the GT governor reduces the fuel mass flow in the GT combustor in order to preserve the GT components from overloads or over-temperatures.

4.2. Ship propulsion plant simulator validation

The described simulation model has been validated comparing the simulation results with sea trials data, measured during the on board test campaign of the vessel, referred to steady state load conditions for different telegraph lever positions. The errors between numerical and experimental data are shown in [Table 1](#) and have been considered acceptable for all monitored parameters, particularly at high engine loads.

5. Monitoring and diagnosis code development

A computer code has been developed for the frigate propulsion plant monitoring purposes, based on the computation of the MD value of a given set of measured variables in order to quantify the abnormality of the current working condition of the system. If an abnormal condition is detected, diagnosis is performed using an ANN. The monitoring and diagnosis system is briefly described in this paragraph.

5.1. MD based monitoring

A useful set of parameters ([Table 2](#)) has been selected in order to obtain information about the health state of the system. The variables selection has been performed on the basis of the results obtained by the authors in previous works ([Campora et al., 2015](#); [Zaccone et al., 2015](#)) by analyzing the simulator's behavior with Design of Experiments (DoE) techniques, in order to underline the major mutual influences between the parameters of the problem.

Table 1 Errors [%] between simulation and sea trials data.

Telegraph lever pos. [%]	38	47	67	80	90
	[%]	[%]	[%]	[%]	[%]
GT power	-0.27	-0.19	0.11	-0.56	0.01
GT speed	1.32	0.87	1.05	0.94	2.35
GG speed	-1.15	-0.12	1.15	0.35	0.45
Compressor exit temp.	11.63	7.94	4.61	4.35	2.32
GG exit temp.	-11.46	-10.9	-9.85	-7.94	-3.22
Fuel mass flow rate	-2.20	-1.75	-3.28	-3.52	-2.20
Ship speed	-2.08	1.78	-2.33	-0.40	2.18
Propeller thrust	-2.43	1.30	1.84	1.13	1.93

Note also that the air temperature is not included in [Table 2](#), despite it is expected to significantly affect the plant performances. Later in the paper, results will show that the knowledge of this parameter is not necessary to the MD monitoring system to discriminate between healthy and unhealthy conditions of the propulsion plant. The reference database for the 'healthy' condition has been generated via simulation. An acceptability interval has been defined for each simulator's fault coefficient, on the basis of practical considerations; the obtained multivariate domain, assumed as representative of the normal operating condition, has been sampled by using Sobol quasi-random space filling sequence in order to generate the reference space (MS) and to capture the correlation effects between the variables. In particular, 200 points have been computed. The mean and standard deviation vectors, **m** and **s** respectively, and the correlation matrix **C** have been computed, in order to calculate the MD values of the MS elements and future conditions. If a generic pattern **X** is given, MD can be evaluated according to (3), where **Z** is the standardized pattern obtained by the (2). As said earlier, a high MD value is a symptom of an abnormal condition. MD values for MS individuals are shown in [Fig. 6](#), where the line represents the unitary mean of MDs. Note that MD values of MS elements, which are representative of the normal condition, are close to 1.

5.2. Diagnostic ANN

In [Campora et al. \(2015\)](#), the authors presented the development of a diagnostic neural network for the here considered case study, based on simulation data. For the presented application, an inverse ANN is designed to compute the diagnostic parameters from a set of measured state variables, and it is based on the inversion of the simulator's input/output relationship.

The propulsion plant simulation model has 16 input variables (fault coefficients): input parameters, listed and described in [Campora et al. \(2015\)](#); they are the telegraph lever position, the air

Table 2 List of monitored parameters.

1	<i>p_1</i>	Compressor inlet pressure
2	<i>p_2</i>	Compressor outlet pressure
3	<i>T_2r</i>	Compressor outlet pressure
4	<i>n_gg</i>	Gas generator shaft speed
5	<i>M_f</i>	Fuel mass flow rate
6	<i>p_4</i>	Low pressure turbine inlet pressure
7	<i>T_5</i>	Low-pressure turbine inlet temperature
8	<i>p_6</i>	LP turbine outlet pressure
9	<i>T_6</i>	LP turbine outlet temperature
10	<i>M_1</i>	Total mass flow rate
11	<i>Q_GT</i>	LP turbine torque
12	<i>Q_PropPort</i>	Propeller torque (portside)
13	<i>Q_PropStbd</i>	Propeller torque (starboard side)
14	<i>TH_PropPort</i>	Propeller thrust (portside)
15	<i>TH_PropStbd</i>	Propeller thrust (starboard side)
16	<i>V_ship</i>	Ship speed

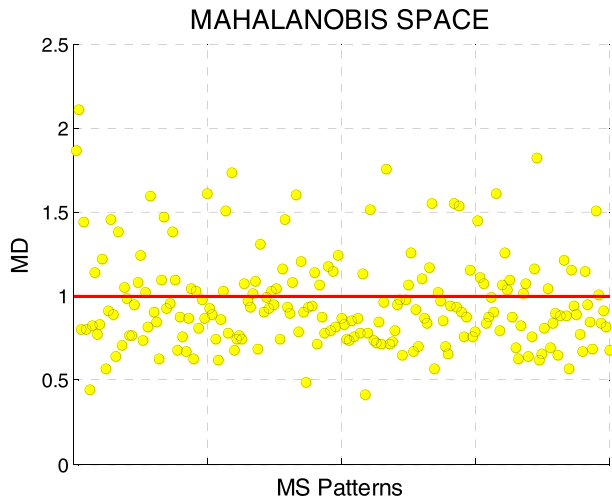


Fig. 6. MD of the MS elements.

temperature and pressure, the gas turbine fault coefficients (inlet, compressor, high and low pressure turbine, outlet and mechanical friction losses coefficients), the shaft lines coefficients (bearing friction increase, propeller thrust and torque coefficients) and the hull roughness increase coefficient. The simulation is based on the solution of thermodynamic and physical equations, so almost any intermediate variable of the simulation process can be chosen as simulator's output. In order to make the study more realistic, a set of measurable variables has been initially selected, on the basis of practical considerations (for example technological limitations in variables real measurement). Maximum and minimum values for each fault coefficient has been set on the basis of previous works (Campora et al., 2015) in order to match the performance decay associated with approximately 2 years of operation for the hull and propeller, and 14000 h for the machinery. A DoE analysis of the input multivariate domain has been carried out to point out the mutual influences between the variables: the domain has been pseudo randomly filled with 1500 points according to Sobol's sequence, then Student's t-test has been used in order to choose the optimal set of variables to characterize a generic plant fault condition. Also, the simulator input parameters (fault coefficients) have been rearranged in order to obtain a more suitable set of output diagnostic parameters. The database obtained by DoE analysis is an exhaustive description of the response of the simulation model in any fault condition and has been used as a training set for the diagnostic network. A more detailed description of the procedure is provided in Campora et al. (2015). The final input and output parameters of the diagnostic network are summarized in Tables 3 and 4.

Data availability is a crucial issue in ANN training. A simulation model can be useful to provide data, however, a direct comparison between experimental and simulation data can lead to serious errors. A simple solution to this problem is a calibration of the input data of the training set on the basis of a known set of experimental measures, typically referred to the new ship. If the variable X is considered, calibration is made in accordance with the following:

$$X_{calibrated} = \frac{X_0_{measured}}{X_0_{model}} X_{model} \quad (5)$$

Typically, ANN input/output variables are normalized to [0; 1] or [-1; 1]. If the ANN is trained with normalized data the calibration is limited to the maximum and minimum value of the variables. The proposed correction methods are now under authors' extensive testing on the basis of experimental data.

Table 3
Diagnostic ANN input variables.

Input	
T_C	air temperature
p_1	Compressor inlet pressure
p_2	Compressor outlet pressure
T_{2r}	Compressor outlet pressure
n_{gg}	Gas generator shaft speed
M_f	Fuel mass flow rate
p_4	Low pressure turbine inlet pressure
T_5	Low-pressure turbine inlet temperature
p_6	LP turbine outlet pressure
T_6	LP turbine outlet temperature
M_1	Total mass flow rate
Q_{GT}	LP turbine torque
$Q_{PropPort}$	Propeller torque (portside)
$Q_{PropStbd}$	Propeller torque (starboard side)
$TH_{PropPort}$	Propeller thrust (portside)
$TH_{PropStbd}$	Propeller thrust (starboard side)
V_{ship}	Ship speed

Table 4
Diagnostic ANN output variables.

Output	
K_{pin}	Compressor inlet filter fault coefficient
K_{Cm}	Compressor fault coefficient
K_{THP}	HP turbine fault coefficient
K_{TLP}	LP turbine fault coefficient
$K_{HullRes}$	Hull resistance increase coefficient
F_{Prop}	Propeller fault coefficient
η_{TR}	Transmission mechanical efficiency

6. Results

In this first application of the presented monitoring and diagnostics procedure, the plant components fault coefficients are varied one by one in their ranges (Campora et al., 2015), in order to test the sensibility of the method and validate the Mahalanobis Distance scale. The variation ranges are referred to 6000 h of operation for the machinery and 700 days for hull and propeller. The state parameters percentage variation plots at fixed degradation percentages are reported in a radar chart. Also, Mahalanobis distance vs percentage degradation curve and fault coefficients radar plots at fixed degradation percentages are reported, the last obtained as ANN output and normalized in [0,1] interval, 0 referring to complete degradation (100% degradation in figures legend) and 1 to maximum health (0% degradation in figures legend).

6.1. Inlet air filter degradation

The inlet filter is designed to protect the gas turbine components from dust, particles, salty water drops and any other impurity, which can affect gas turbine integrity and correct operation. Usually, the air filter is cleaned or changed more when a threshold pressure drop is reached, in order not to affect the gas generator performance.

Filter degradation is simulated increasing K_{pin} coefficient (Fig. 9). Note that in this particular case, as a consequence of the above-reported convention, the value 1 in normalized scale is associated with the minimum value of K_{pin} coefficient, while the value 0 (maximum degradation) is associated to the maximum. The principal effect is a pressure drop in the inlet section (p_1), which influences the entire gas path, while no effects are observed on ship speed, which is held constant by the governor (Fig. 7). Note that the coefficient variation range considered has been set in order to get an operationally reasonable pressure drop. The MD increase due to degradation has a linear behavior (Fig. 8).

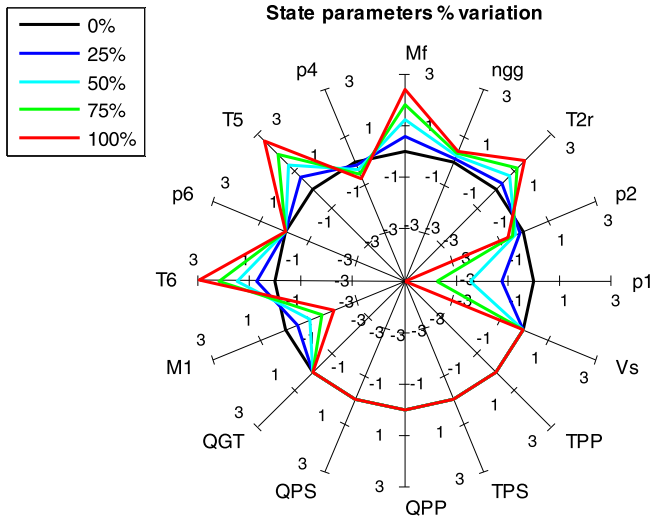


Fig. 7. Inlet air filter degradation: state parameters % variation.

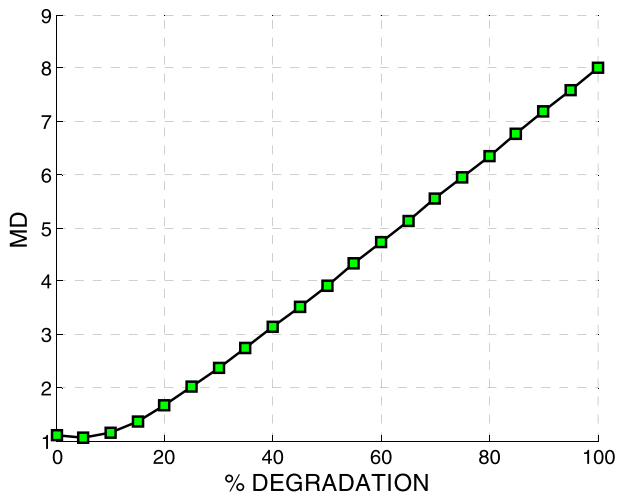


Fig. 8. Inlet air filter degradation: MD increase.

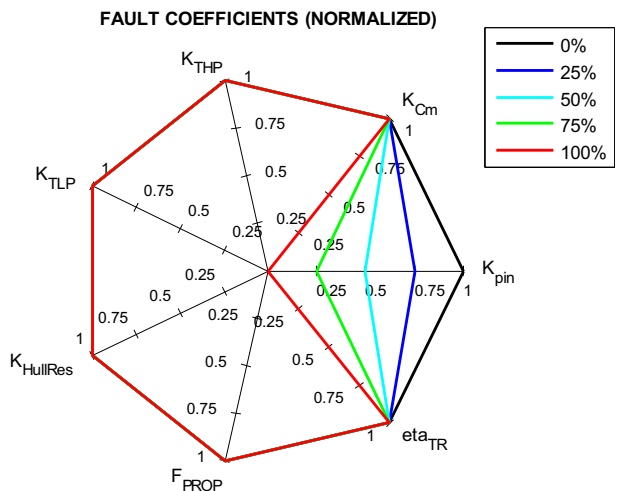


Fig. 9. Inlet air filter degradation: ANN output.

6.2. Compressor degradation

Compressor degradation is mainly due to dust, insects, pollens, which are not trapped by the filter and stick to the compressor blades, reducing the efficiency and mass flow rate.

The compressor is degraded by K_{Cm} coefficient decrease. Again, the efficiency and mass flow rate reduction have heavy effects on all the gas path, while no ship speed reduction is observed (Fig. 10). MD increase is linear (Fig. 11), and a small error is observed in Diagnostic ANN output (Fig. 12).

6.3. Turbine degradation

Turbine efficiency degradation is due to contaminant agents coming from the combustor, mainly NOx, fuel particles, fuel additives. In this case, HP and LP turbines degradation is simulated (Fig. 15): all the pressure values upstream of the turbine sections increase, and an increased fuel consumption is observed (Fig. 13). MD increases again with a linear behavior (Fig. 14).

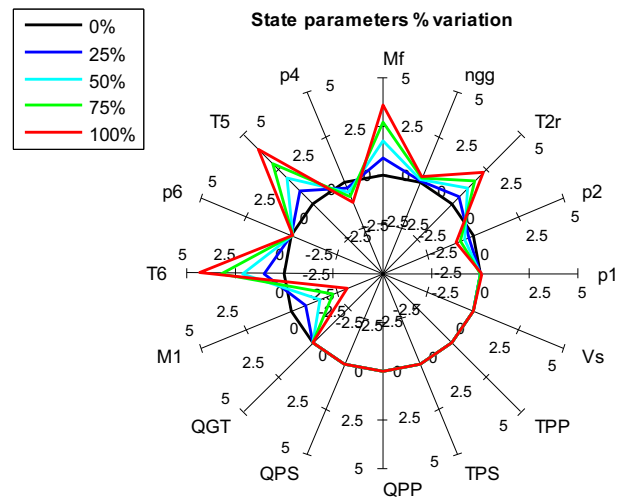


Fig. 10. Compressor degradation: state parameters % variation.

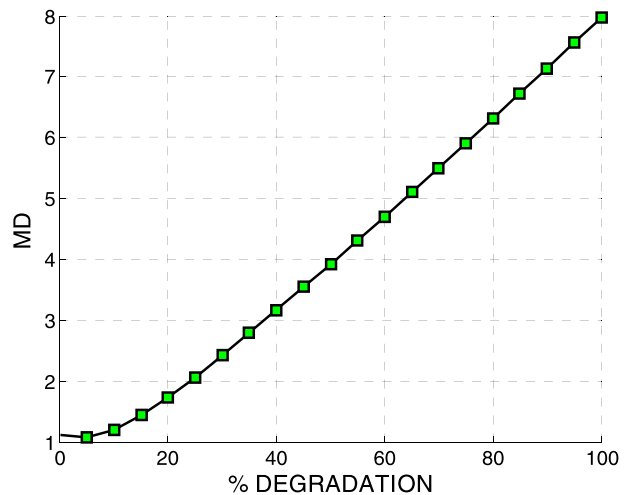


Fig. 11. Compressor degradation: MD increase.

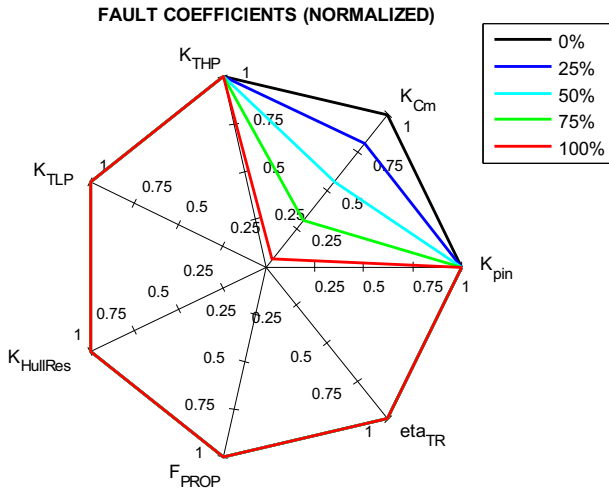


Fig. 12. Compressor degradation: ANN output.

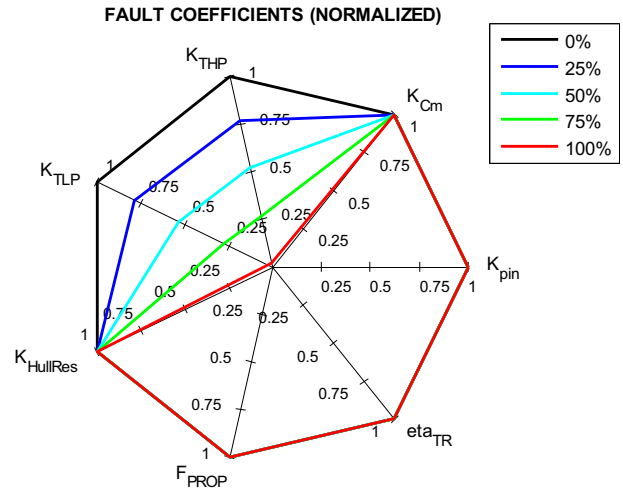


Fig. 15. Turbine degradation: ANN output.

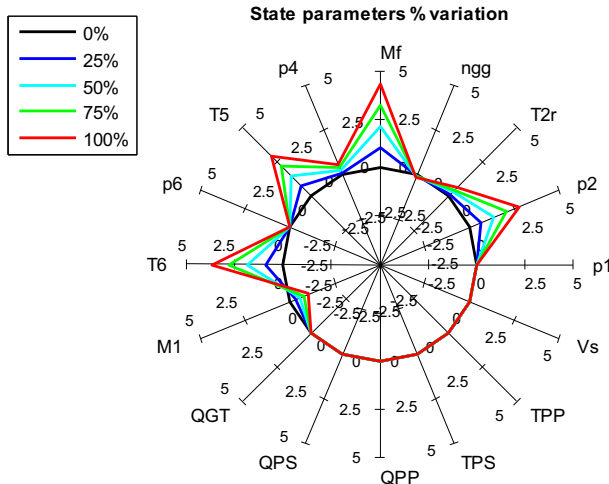


Fig. 13. Turbine degradation: state parameters % variation.

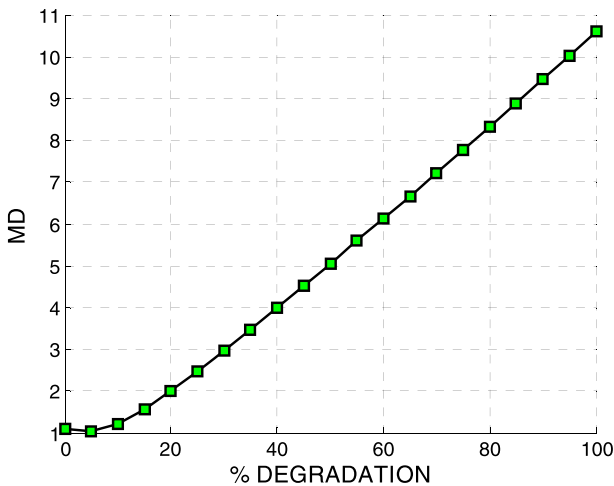


Fig. 14. Turbine degradation: MD increase.

6.4. Hull degradation

Hull roughness increases in time, especially during long inactivity periods: this is mainly due to corrosion and biological deposits (fouling).

Hull roughness increase is simulated by $K_{HullRes}$ coefficient (Fig. 18), which acts on an additive hull resistance component: in this case, ship speed decreases, while propeller thrust and torque and fuel consumption increase (Fig. 16). Note that the obtained ship speed is a consequence of the ship propulsion governor logic that matches the equilibrium between propeller and hull, which performance parameters have been varied by degradation. MD increases with a slightly more than linear behavior (Fig. 17).

6.5. Propeller degradation

Similarly to the previous case, the propeller is affected by fouling, causing a reduction of propeller efficiency (i.e. thrust loss and a torque increase), which is operated by F_{prop} coefficient in the model (Fig. 21). This coefficient controls both the thrust reduction and torque increase coefficients introduced in section 3. This simplification is necessary in order to avoid numeric issues in

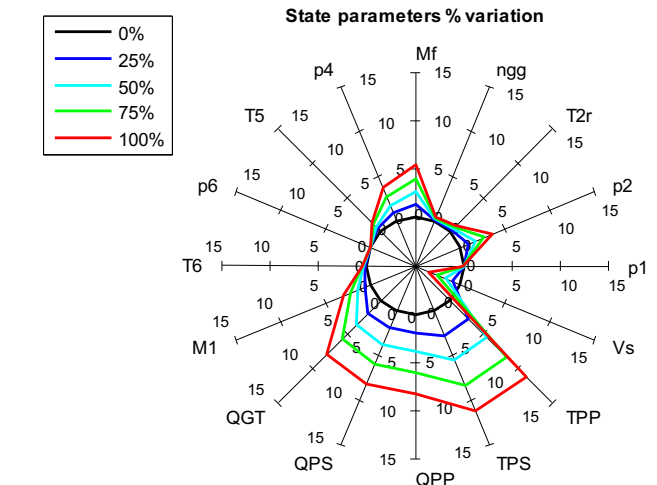


Fig. 16. Hull fouling: State parameters % variation.

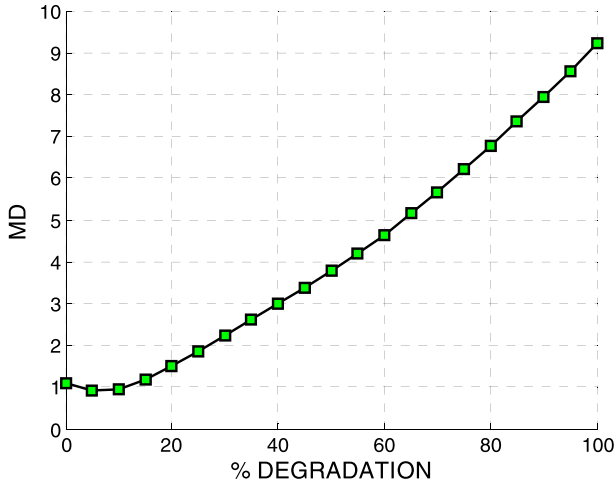


Fig. 17. Hull fouling: MD increase.

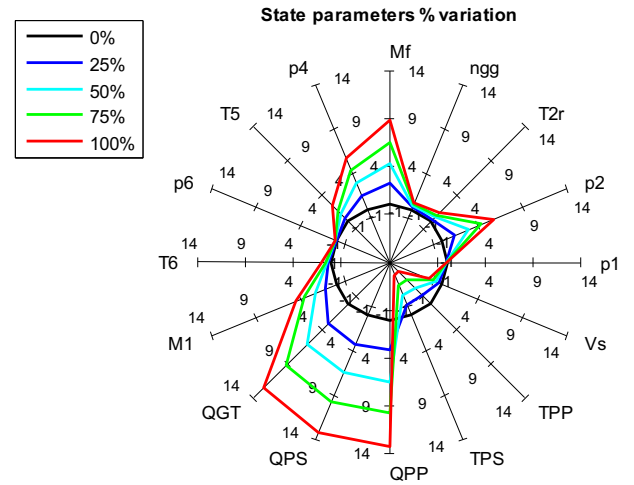


Fig. 19. Propeller fouling: State parameters % variation.

diagnostic ANN training (Campora et al., 2015). As opposed to the previous case, propeller degradation makes the thrust drop together with ship speed, while torques and fuel consumption increase (Fig. 19). MD behavior is again not linear (Fig. 20).

6.6. Combined fault cases

Two examples of multiple faults are now studied. For each case, the degradation is progressively increased through fault coefficients in order to simulate in-time performance decay. The considered cases are the following:

- 1) GT fault: inlet filter, compressor, and turbine are affected by progressive degradation.
- 2) Hull and propeller fouling: progressive increase of friction is simulated for the components subject to sea water fouling and corrosion.

Diagnostic results are reported in Figs. 22–27. The overall health state of the plant is monitored through MD. When MD value exceeds a threshold value, fault coefficients can be computed by the ANN, in order to make the diagnosis. For each case, MD versus time is reported. A threshold value for MD needs to be chosen, on the

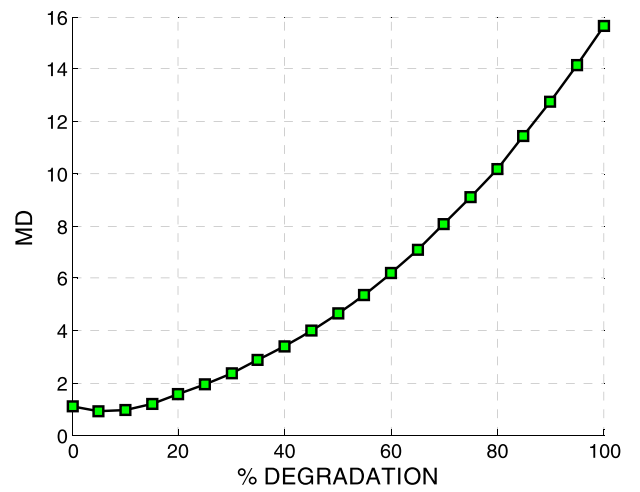


Fig. 20. Propeller fouling: MD increase.

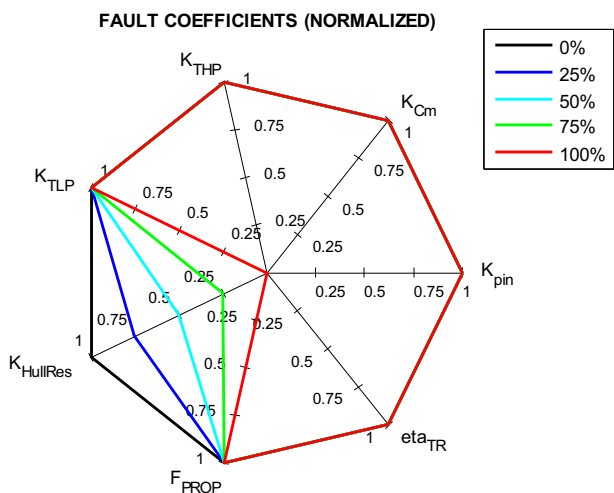


Fig. 18. Hull fouling: ANN output.

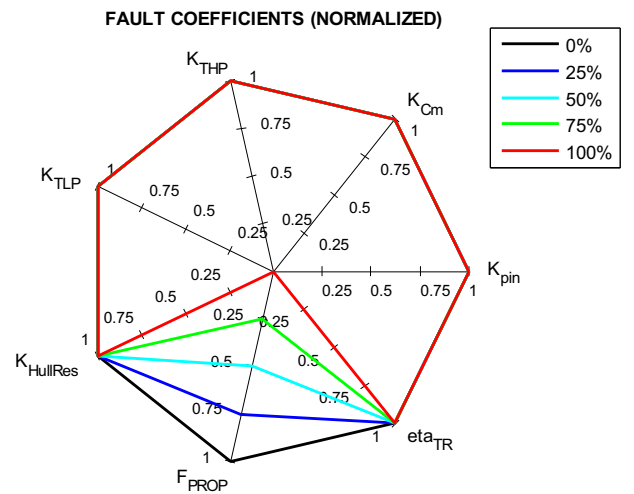


Fig. 21. Propeller fouling: ANN output.

basis of ship's performance decay acceptance ranges. The value 5 is chosen here as an example: threshold value selection is crucial in

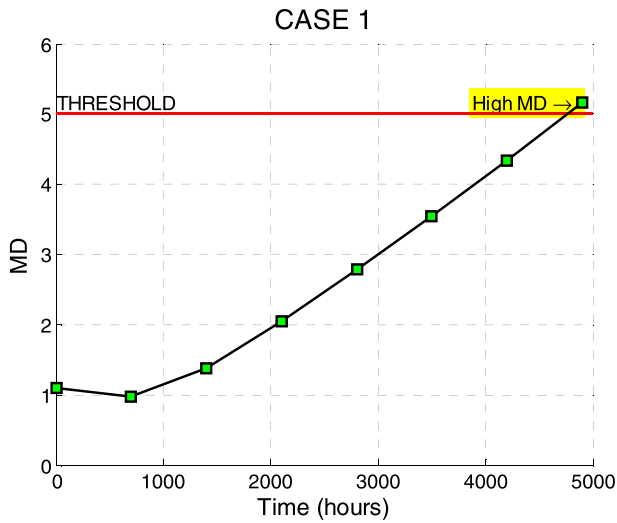


Fig. 22. Case 1: fault detection via MD monitoring

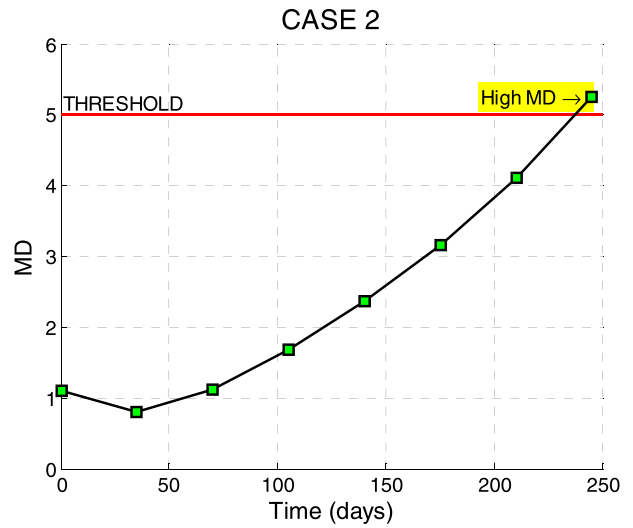


Fig. 25. Case 2: fault detection via MD monitoring.

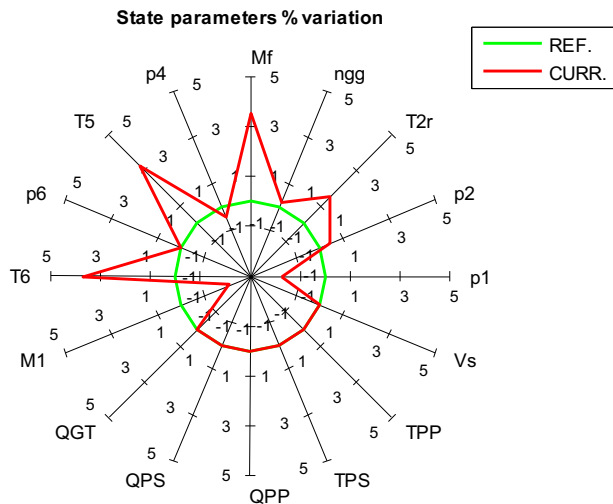


Fig. 23. Case 1: State parameters % variation.

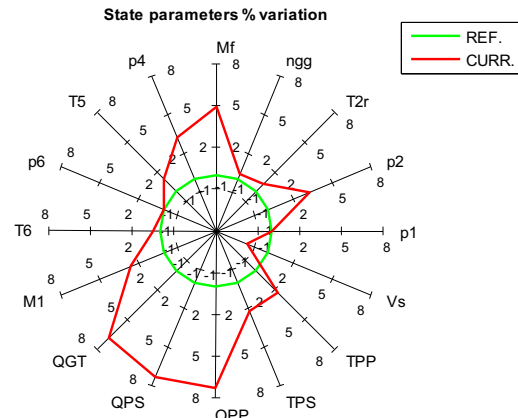


Fig. 26. Case 2: state parameters % variation.

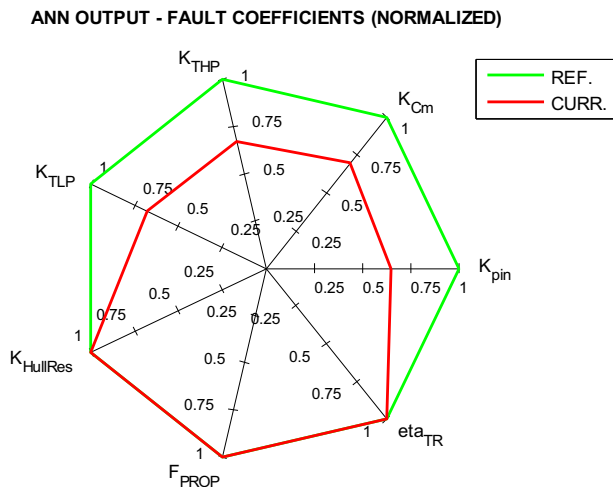


Fig. 24. Case 1: ANN output.

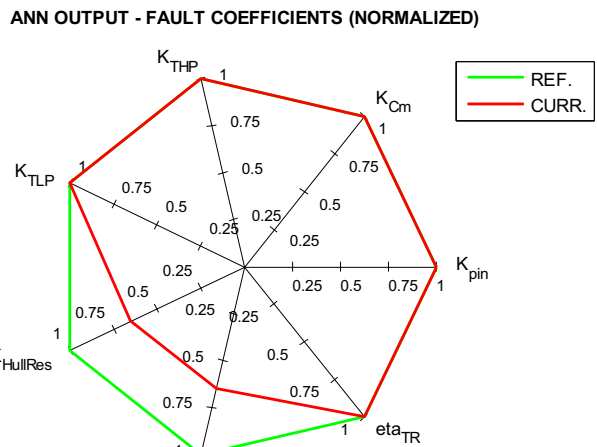


Fig. 27. Case 2: ANN output.

order to provide reliable abnormality detection (Taguchi and Jugulum, 2002). When MD exceeds the value 5, fault coefficients

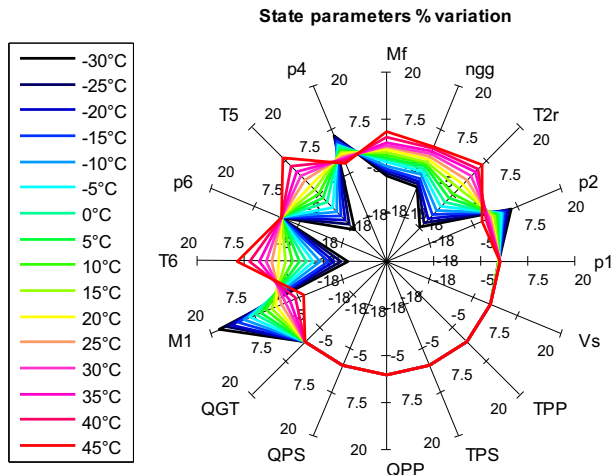


Fig. 28. Air temperature influence: state parameters % variation.

are calculated by the ANN, normalized to [0; 1], and reported in a radar chart. In addition, State variables performance variations are reported in a second radar chart. In both cases, a significant degradation state is observed, while state parameters variations are relatively limited: In case 1, a high MD (above 5) is detected after 5500 h. The corresponding state parameters variations are below 3%. Neural Network output shows that the GT components are degraded to about 60% of the considered acceptance range. In case 2 a high MD value is detected after about 240 days. The NN output shows that degradation is about 60%. Ship speed decreases of about 1%, while fuel mass flow rate is increased by 5%.

6.7. External temperature influence

Finally, external temperature influence on MD and state parameters is considered, in order to verify the robustness of the system to external conditions changes. Note in fact that the air temperature, despite its significant effect on the plant performances, is not monitored (Table 2). A wide range of temperatures has been analyzed, from -30 °C to 45 °C, corresponding to the ship’s mission requirements. Fault coefficients correspond to maximum health in all the cases, so are omitted. Results are reported in Figs. 28 and 29: MD values are far from the threshold

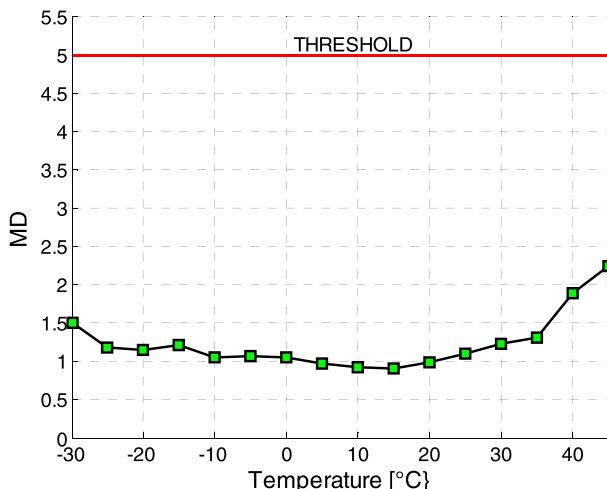


Fig. 29. Air temperature influence: MD.

value even at extreme values of the temperature range, while state parameters of the gas path are subject to heavy variations. This result suggests that state parameters monitoring is not an effective way to recognize abnormal conditions of the GT without correlations.

7. Conclusions

An approach to power plants monitoring and diagnostics has been presented in this paper, combining simulation techniques, artificial neural networks and a Mahalanobis Distance based monitoring method. An application example to a marine gas turbine powered propulsion plant has been described. A simulation model of the plant has been used in order to generate data in different fault conditions, in order to train a diagnostic neural network and create a reference set of measures for Mahalanobis Distance calculation. The MD has been used as a global index to identify the health state of the system, while more detailed diagnosis has been carried out on the basis of an ANN diagnostic metamodel. In addition, a calibration procedure has been proposed in order to make better use of simulation data in ANN training. A full validation of the proposed calibration is currently under authors’ research. Single and multiple fault cases have been analyzed. In all the considered cases MD monitoring has been a useful tool for early detection of the faults, in particular, those related to gas turbine components, that lead to hardly recognizable and relatively small changes in the monitored state parameters if compared to the ones associated to external temperature variations. For demonstrative purposes, a threshold value has been set for ANN intervention for more detailed diagnosis. In real applications, the threshold value should be selected based on ship performance evaluation compared to mission requirements.

References

Altosole, M., Martelli, M., 2017. Propulsion control strategies for ship emergency manoeuvres. *Ocean. Eng.* 137 (2017), 99–109.

Altosole, M., Benvenuto, G., Campora, U., 2010. Numerical modelling of the engines governors of a CODLAG propulsion plant. In: 20th BLACK-SEA International Congress, Varna, Bulgaria, 7–9 October.

Altosole, M., Martelli, M., Vignolo, S., 2012a. A mathematical model of the propeller pitch change mechanism for the marine propulsion control design. In: Rizzuto, Soares, Guedes (Eds.), *Sustainable Maritime Transportation and Exploitation of Sea Resources*, vol. II, pp. 649–656.

Altosole, M., Figari, M., Martelli, M., 2012b. Time domain simulation for marine propulsion applications. In: *Proceedings of the 2012-Summer Computer Simulation Conference, SCSC 2012, Part of SummerSim 2012 Multiconference*. Genoa, Italy, 8–11 July.

Altosole, M., Campora, U., Martelli, M., Figari, M., 2014. Performance decay analysis of a marine gas turbine propulsion system. *J. Ship Res.* 58 (3) <https://doi.org/10.5957/JOSR.58.3.130037>. September 2014, pp. 117–129, ISSN:0022-4502.

Benvenuto, G., Campora, U., 2005. A gas turbine modular model for ship propulsion studies. In: *HSMV, 7th Symposium on High Speed Marine Vehicles*. Naples, Italy, 21 – 23 September.

Benvenuto, G., Campora, U., Carrera, G., Figari, M., 2000. Simulation of ship propulsion plant dynamics in rough sea. In: *8th International Conference on Marine Engineering Systems (ICMES/SNAME 2000)*. New York, USA, May 22–23.

Bidini, G., Grimaldi, C.N., Mariani, F., 1998. Un approccio non convenzionale per la diagnosi di motori di notevole dimensione. In: *53^o Congresso Nazionale A.T.I.* Florence, Italy, September 15–18.

Campora, U., Carretta, M., Cravero, C., 2013. Performance decay simulation of a gas turbine for helicopter propulsion. *Transaction Control Mech. Syst.* 2, 105–114. March.

Campora, U., Capelli, M., Cravero, C., Zacccone, R., 2015. The development of meta-models of a gas turbine powered marine propulsion system for simulation and diagnostic purposes. *J. Nav. Archit. Mar. Eng.* 12 (No 1, June), 1–14. <https://doi.org/10.3329/jname.v12i1.19719>. ISSN 1813-8535 (Print), 2070-8998 (Online).

Coraddu, A., Oneto, L., Ghio, A., Savio, S., Anguita, D., Figari, M., 2016. Machine learning approaches for improving condition-based maintenance of naval propulsion plants. *Proc. Institution Mech. Eng. Part M J. Eng. Marit. Environ.* 230 (1), 136–153.

Fentaye, A.D., Gilan, S.I.U.H., Baheta, A.T., 2016. Gas turbine gas path diagnostics: a review. In: *MATEC Web of Conferences*, vol. 74. EDP Sciences, p. 00005.

- Cohen, H., Rogers, G.F.C., Saravanamuttoo, H.I.H., 1987. Gas Turbine Theory, third ed. Longman Scientific & Technical, Harlow, Essex, England.
- Haykin, S., 1998. Neural Networks: a Comprehensive Foundation. Prentice Hall PTR, Upper Saddle River, NJ, USA. ISBN:0132733501.
- Izadi-Zamanabadi, R., Blanke, M., Katebi, S., 2001. Cheap Diagnosis Using Structural Modeling and Fuzzy Logic Based Detection. Elsevier. August 19.
- Kramer, M.A., 1991. Nonlinear principal component analysis using auto-associative neural networks. AIChE J. 37 (February), 233–243.
- Kumano, S., Aoyama, K., Mikami, N., 2011. Advanced Gas Turbine Diagnostics Using Pattern Recognition. ASME paper GT2011–45670.
- Li, Y.G., 2002. Performance analysis based gas turbine diagnostics: a review. Proc. Institution Mech. Eng. Part A: J. Power Energy 216 (5, September), 363–377.
- Li, P., Su, B., 2008. On the intelligent fault diagnosis methods for marine diesel engine. In: ICACIA International Conference on Apperceiving Computing and Intelligence Analysis, Chengdu, pp. 397–400. E_ISBN: 978-1-4244-3426-8.
- Martelli, M., Viviani, M., Altosole, M., Figari, M., Vignolo, S., 2014a. Numerical modelling of propulsion, control and ship motions in 6 degrees of freedom. J. Eng. Marit. Environ. 228 (4), 373–397.
- Martelli, M., Figari, M., Altosole, M., Vignolo, S., 2014b. Controllable pitch propeller actuating mechanism, modelling and simulation. J. Eng. Marit. Environ. 228 (1), 29–43.
- Michetti, S., Ratto, M., Spadoni, A., Figari, M., Altosole, M., Marcelli, G., 2010. Ship Control system wide integration and the use of dynamic simulation techniques in the Fremm project. In: Proceedings of the International Conference on Electrical Systems for Aircraft, Railway and Ship Propulsion, ESARS'10, Bologna, Italy, October 19–21.
- Ogaji, S.O.T., Marinai, L., Sampath, S., Singh, R., Prober, S.D., 2005. Gas-turbine fault diagnostics: a fuzzy logic approach. Appl. Energy 82 (1), 81–89.
- Palmé, T., Breuhaus, P., Assadi, M., Klein, A., Kim, M., 2011a. New Alstom Monitoring Tools Leveraging Artificial Neural Network Technologies. ASME paper GT2011 – 45990.
- Palmé, T., Breuhaus, P., Assadi, M., Klein, A., Kim, M., 2011b. Early Warning of Gas Turbine Failure by Nonlinear Feature Extraction Using an Auto-associative Neural Network Approach. ASME paper GT2011–45991.
- Pawletko, R., 2005. The use of neural networks for the faults classification of a marine diesel engine fuel injection system. UICEE. Glob. J. Engng. Educ. 9 (9) published in Australia.
- Rigoni, E., Lovison, A., 2007. Automatic Sizing of Neural Network for Function Approximation. International Conference on Systems, Man and Cybernetics, ISIC, IEEE, Montreal, Canada.
- Stamatis, A.G., 2011. Evaluation of gas path analysis methods for gas turbine diagnosis. J. Mech. Sci. Technol. 25 (2), 469.
- Taguchi, G., Jugulum, R., 2002. The Mahalanobis – Taguchi Strategy: a Pattern Technology System, fifth ed. John Wiley & Sons. ISBN: 978-0-471-02333-3.
- Urban, L.A., 1969. Gas turbine engine parameter interrelationships. In: Hamilton Standard Division of United Aircraft Corporation, second ed.
- Verbist, M.L., Visser, W.P.J., P van Buijtenen, J., Dulvis, R., 2011. Gas Path Analysis on KLM I In-flight Engine Data. ASME paper GT2011–45625.
- Zaccone, R., 2013. Monitoraggio di un impianto di propulsione navale con turbina a gas mediante simulazione e metamodelli. Marine Engineer & Naval Architect Graduate Thesis. University of Genoa, Politechnic School, Dipartimento di Ingegneria Navale, Elettrica, Elettronica e delle Telecomunicazioni (DITEN), Italy. July 19, in Italian.
- Zaccone, R., Altosole, M., Campora, U., Figari, M., 2015. Diesel engine and propulsion diagnostics of a mini-cruise ship by using artificial neural networks. In: Proc. Of the 16th International Congress of the International Maritime Association of the Mediterranean, Pula (Croatia), 21–24 September.